

Simulation of the Potential Responses of Regional Climate and Surface Processes in Western North America to a Canonical Heinrich Event

S.W. Hostetler

U.S. Geological Survey, Corvallis, Oregon

P.J. Bartlein

Department of Geography, University of Oregon

We apply a hierarchy of atmospheric and process models to assess the response in Western North America to a canonical North Atlantic Heinrich event that is characterized by lowering of the Laurentide Ice Sheet (LIS) and subsequent warming of North Atlantic sea surface temperatures (SSTs). Global responses to changes in the LIS and SSTs are simulated by the GENESIS general circulation model. Lateral boundary conditions for a high-resolution regional climate model (RegCM) that is run over Western North America are derived from the GENESIS simulations, and output from the RegCM simulations is used as input to a suit of models that we apply to investigate responses of alpine glaciers, lakes, vegetation, and coastal upwelling. The combined expression of synoptic- and regional-scale circulations yields spatially variable climatologies over WNA in each phase of our H2 event that reinforce, cancel, or reverse climatic patterns (e.g. temperature and precipitation) of previous phases. The response of terrestrial and marine processes is complex, and illustrates the possibility of spatially heterogeneous registration of millennial-scale climatic variations both within a particular phase and among the various phases of those variations.

1. INTRODUCTION

Over the past 50,000 years, the climate of western North America (WNA) has varied on both orbital or Milankovitch time scales and on higher frequency millennial time scales [Clark and Bartlein, 1995; Behl et al, 1996; Benson et al.,

1996; Philips et al., 1996; Oviatt, 1997; Benson et al., 1998; Lund and Mix, 1998]. Although the mechanisms of orbital-scale forcing of climatic changes in this region are relatively well understood [Whitlock and Bartlein, 1997; Thompson et al., 1993], our knowledge of the mechanisms associated with millennial-scale climatic variations is less complete. A prominent question regarding climatic variability on the millennial scale is whether and how the relatively abrupt variations, such as those accompanying North Atlantic Heinrich events, were propagated to WNA. Conceptually, there are three pathways by which such millennial scale variations could become registered in

Mechanisms of Global Climate Change at Millennial Time Scales
P.U. Clark, R.S. Webb, and L.D. Keigwin (eds.)
Geophysical Monograph 112
American Geophysical Union (1999), pp. 313-327

WNA: 1) through atmospheric or oceanic transmission from the North Atlantic region, 2) through a joint response of the coupled ocean-atmosphere system, or 3) through some combination of both [Clark and Bartlein, 1995]. In an example of the propagation of a North Atlantic “signal” via the first pathway, a climatic variation in the North Atlantic region might perturb the atmospheric general circulation or ocean thermohaline circulation. This perturbation in turn might produce regional climatic changes throughout the globe as effects of the circulation changes propagated along their flow paths. In an example of propagation via the second pathway, climatic variations in both the North Atlantic region and WNA would be viewed as the regionally specific responses to some large- (hemispheric or global) scale forcing.

Insights into the nature of propagation along either of the two main pathways can be obtained through modeling. Features of the regional climatic response consistent with joint dependence or the atmospheric transmission of a Heinrich event can be isolated through a straightforward series of simulations in which appropriate changes to the relevant, large-scale boundary conditions [i.e., height of the Laurentide ice sheet (LIS) and North Atlantic sea surface temperatures (SSTs)] are prescribed [Hostetler *et al.*, 1999], and such an approach forms the core of this paper. Modeling the transmission via ocean circulation, or the joint response to ocean-atmosphere interactions during millennial-scale climate variations, is much more complex and requires an earth system model in which the various subsystems, the atmosphere, terrestrial biosphere, land surface, cryosphere, and oceans, are interactively coupled. The full earth-system model required for such an analysis does not yet exist.

The local- and regional-scale variations in surface processes and environmental systems that are recorded by paleoclimatic indicators are generated by a hierarchy of controls and responses that span multiple temporal and spatial scales. Hemispheric- and synoptic-scale atmospheric and oceanic circulation systems are controlled by global boundary conditions such as latitudinal and seasonal distributions of insolation, patterns of SSTs, and the size and distributions of continental ice sheets. Global circulation systems in turn govern regional or mesoscale circulations (those occurring on a spatial scale on the order of tens of kilometers) which in turn are modified by more localized features such as topographic barriers, large lakes, and coastline orientation. Although climatic features at all scales are important, substantial insights into the climate of WNA can be obtained by extracting and quantifying the relative contributions of synoptic-scale features and the expression of those features at the regional scale. In WNA, the primary regional scale influence on synoptic circulations is exerted by complex topography. Topographic effects on atmospheric circulation are characterized, for example, by blocking and channeling of winds, generation of orographic precipitation, and

modification of latitudinal temperature gradients. These topographic effects, in turn, strongly influence the distribution and nature of surface water, vegetation and alpine glaciers, and thus the geologic records of changes in these systems.

Models of the general circulation of the atmosphere (AGCMs) provide simulations of large-scale atmospheric circulation, but many circulation features at the regional scale are not explicitly resolved by AGCMs, which typically are run at a horizontal grid spacing of several degrees for climate simulations (Figure 1). For the purposes of explicitly representing the various scales of controls and responses in WNA involved in the atmospheric transmission of a Heinrich event in the North Atlantic region, we designed a climate-modeling experiment based on a hierarchy of atmospheric and process models. A series of simulations of global climate were conducted with the GENESIS AGCM to evaluate large-scale atmospheric responses to three phases of a canonical representation of Heinrich event 2 (H2) (Hostetler *et al.*, 1999). GENESIS has an effective resolution for atmospheric variables of 3.75 degrees, and for land-surface variables of 2 degrees (or grid-square areas of approximately $12.0 \times 10^4 \text{ km}^2$ and $3.4 \times 10^4 \text{ km}^2$, respectively, at 45°N) (Figure 1). From the GENESIS simulations, we derived time series of the necessary lateral boundary conditions for a regional (mesoscale) climate model (the NCAR RegCM) that was run at a grid spacing of 60 km over WNA. The model hierarchy is completed by using output fields from the RegCM to infer vegetation responses, and as input to a series of models that quantify glacier mass balance, surface water balance, lake levels, and lake thermal response, and coastal upwelling, to the canonical Heinrich event.

2. EXPERIMENTAL DESIGN

In a previous study [Hostetler *et al.*, 1999], we used GENESIS to assess the global atmospheric and surface response to three phases of a canonical Heinrich event patterned after the ice sheet and SST variations that accompanied event H2. In phase one, nominal 21 ka boundary conditions are prescribed that include CLIMAP SSTs [CLIMAP Project Members, 1981], continental ice sheets [Peltier, 1994], and appropriate orbital parameters and atmospheric composition (CO_2 concentration of 200 ppmv). In the following discussion, this simulation is designated *MaxCold*. Phase one of the canonical event is followed by phase two in which a surge of the LIS into the North Atlantic is represented by lowering the LIS in our model from the maximum 21 ka height to a height ~1500 m lower over Hudson Bay [Licciardi *et al.*, 1998], and is designated *MinCold*. In phase three, designated *MinWarm*, the lower LIS is accompanied by a uniform increase of North Atlantic SSTs north of 30°N to values three fourths of the way between full glacial and modern temperature

[Cortijo *et al.*, 1997]. We also include a GENESIS simulation of the present-day climate (designated *Control*) as a reference for comparing the magnitude of Heinrich event responses to those of a glacial-interglacial climate change. Each GENESIS simulation was 15 years long, and the output necessary to derive initial and lateral boundary conditions for the RegCM [surface temperature (including SSTs) and pressure, and vertical profiles of temperature, wind, humidity, and pressure] for 5 years was retained for simulation years 11 through 15.

The version of RegCM used here is based on the standard version that is described by *Giorgi et al.* [1993a, b]. Our version of RegCM includes a) an improved lake submodel [*Small et al.*, in press] for interactive modeling of lake-atmosphere feedbacks, b) a modified method for computing the energy balance and temperature of permanent ice (the mass balance is not computed), c) reduced CO₂ concentration (200 ppmv for 21 ka), and d) calculated solar inputs based on specified values of eccentricity, obliquity and precession. The distributions of vegetation, ice caps and mountain glaciers, the LIS, and pluvial lakes for the regional model domain (Plate 1) are based primarily on published reports [e.g. *Wright et al.*, 1993 and chapters therein], with some modifications (e.g., in the placement of pluvial Lakes Lahontan and Bonneville relative to smoothed model topography). The initial and lateral boundary conditions for the RegCM, which were derived from the GENESIS simulations at 12-hr time steps, begin June 1 and run continuously for 4.5 years. The first half-year of each RegCM run is excluded from our analyses to ensure the model had essentially reached equilibrium.

A suite of process models and computations are used to evaluate the response of surface systems in WNA during the various phases of our H2 event. Glacier mass balance is computed using the temperature and precipitation fields from the RegCM as input to an empirical mass-balance model [*Hostetler and Clark*, 1997]. Lake-level responses are estimated from anomalies of net moisture (precipitation minus evaporation, P-E) from the RegCM and from simulated changes in lake evaporation. Changes in coastal upwelling are computed using the surface wind fields from the RegCM simulations [e.g., *Ortiz et al.*, 1997]. We infer vegetation changes from anomalies of RegCM temperature and effective moisture.

3. RESULTS

We present our results in a “top down” order that parallels the modeling sequence. Discussion of global responses in GENESIS are followed by those for the RegCM and higher resolution process models and computations.

3.1 Global Model

3.1.1 Glacial-Interglacial responses. The glacial-interglacial climate anomalies of our GENESIS experiments (Plate 2, *MaxCold-Control*) are similar to

those for other simulations of the LGM conducted with prescribed CLIMAP SSTs in GENESIS [e.g., *Pollard and Thompson*, 1997], and other AGCMs [e.g., *Manabe and Broccoli*, 1985; *Rind*, 1987; *COHMAP Members*, 1988]. The largest glacial/interglacial temperature differences are found in the northern hemisphere over and to the east of the continental ice sheets, and downwind from areas of colder SSTs (Plate 2a). In both seasons, the *MaxCold* simulation produces steeper temperature gradients between the continents and adjacent oceans than those of the *Control* simulation. Air temperatures in the *MaxCold* experiment are colder over WNA than those of *Control* in both winter and summer; however, the magnitude of winter cooling is less than that of summer (Plate 2a). The smaller winter temperature anomalies stem in part from the *Control* simulation being cold relative to modern observations as a consequence of the improper placement of upper level circulation features in GENESIS (and AGCMs of similar resolution). In contrast to actual conditions, persistent high pressure that forms offshore extends inland over the Great Basin, and anchors the simulated longwave circulation pattern. The anomalous pressure pattern, which is attributable to the use of fixed SSTs and to the resolution of the AGCM, produces air flow over the Great Basin predominantly from a northerly direction which sustains the advection of cold Arctic air into the region.

Changes relative to *Control* in pressure patterns and associated wind fields both at the surface and aloft over WNA are also evident in the *MaxCold* simulation. During the boreal winter of the *MaxCold* simulation, stronger-than-present westerlies are simulated over the northern Pacific in response to a steeper temperature gradient set up by colder air temperatures over the Pacific Northwest (PNW) and North Pacific and a subtropical gyre that is as warm as present (Plate 2b). Thermal and topographic blocking effects of the LIS cause anticyclonic flow over the PNW and splitting and southward displacement of the polar jet stream. The split flow is characterized by a stronger subtropical jet, weaker westerlies along the west coast and south of the Cordilleran ice sheet, and stronger southerly flow into Beringia. A split jet was a common feature in earlier simulations of the LGM climate that were run at low resolution (e.g., R15) with the CLIMAP reconstruction of the LIS [e.g., *Manabe and Broccoli*, 1985; *Rind*, 1987; *COHMAP Members*, 1988]. Subsequent experiments, in which the lower ICE4-G reconstruction of the Laurentide was used, tend to display an evident, but less well developed split jet [*Bartlein et al.*, 1998]. The recurrence of a split jet in our (and other, e.g., *Pollard and Thompson*, 1997) LGM simulations suggests that the feature may reemerge in simulations conducted with higher resolution AGCMs. During summer, westerlies stronger than those of *Control* are simulated in the *MaxCold* experiment, in response to steep temperature gradients between the colder than present Gulf of Alaska and the warmer (>2°C) subtropical gyre.

In the *MaxCold* experiment there is strong wintertime expression of the glacial anticyclone characterized by weaker surface westerlies south of the LIS, prevailing easterlies over the PNW, and a very well-developed Aleutian Low (Plate 2c). Summer flow patterns in the *MaxCold* simulation reflect the combined influences over WNA of the LIS and surface temperature patterns. A prominent anticyclone over the continent (and extending to the North Atlantic), with a diminished subtropical high in the eastern Pacific and a strengthened Aleutian low produce southwesterly flow along the west coast and easterly flow along the edge of the LIS.

The distribution of precipitation (not shown) and P-E anomalies (Plate 2d) reflects the reorganized wind flow over WNA in the *MaxCold* simulation. Anticyclonic flow from the LIS produces off-shore winds over the PNW resulting in winter conditions at the LGM that were colder and drier than present. Precipitation associated with weaker westerlies and a stronger subtropical jet increase P-E from Central America to the southwestern US (SW). Focusing of the polar jet at the latitude of the Cordilleran ice sheet during summer causes wetter-than-present conditions there, while easterly surface winds along the southern edge of the glacial anticyclone advect Gulf moisture into SW and Rocky Mountains.

3.1.2 Heinrich event responses. Lowering the LIS in the second phase of the canonical Heinrich event (*MinCold*) results in cooling over WNA by as much as 4°C in the winter and 2°C in summer (Plate 2a, *MinCold-MaxCold*). The temperature responses are associated with changes in circulation induced by thermal and topographic effects of the lower ice sheet. Relative to the *MaxCold* phase, in the *MinCold* phase in winter lower pressure forms over the Great Basin and higher pressure forms to the east. Winter of the *MinCold* phase is wetter than the LGM (*MaxCold*) in the PNW and drier than the LGM in the SW. Conditions in the PNW in the *MinCold* phase are wetter than those of the *MaxCold* phase because the strength of the easterlies off the LIS is reduced. During summer in the *MinCold* phase, higher pressure than that of the *MaxCold* phase replaces the wintertime low over the Great Basin and lower pressure forms over the eastern Pacific, causing attendant changes in wind flow and moisture. Consequently, summers in the PNW and the SW are wetter in the *MinCold* phase than those of the *MaxCold* phase, with little change elsewhere.

In the third phase of our canonical Heinrich event (*MinWarm* simulation), in which a warm North Atlantic is combined with a low LIS, there is cooling of WNA relative to the *MaxCold* phase, but overall, to a lesser degree than that of the *MinCold* phase (Plate 2a, *MinWarm-MaxCold*). Warmer-than-phase-two temperature anomalies are associated with changes in pressure and circulation patterns (e.g., reduction of the Aleutian Low). Relative to both the *MaxCold* and *MinCold* phases, precipitation and P-E in the *MinWarm* phase decreases over the PNW in winter and increases over the SW during summer.

The climatic response to lowering of the LIS in phase two (*MinCold*) of our H2 event is apparently transmitted to WNA both through changes in the circulation of the northern hemisphere and through circulation changes in North America focused around the LIS. Warming the North Atlantic in phase three (*MinWarm*) causes expected large temperature responses in both the North Atlantic region and downstream over Europe and Asia. Transmission of this response to WNA is primarily accomplished through attendant changes in pressure patterns over the PNW. Temperatures over WNA in the *MinWarm* phase are cooler than those of the *MaxCold* and *MinCold* and P-E is substantially different due to weakening of the Aleutian low and attendant repositioning of wind patterns and storm tracks. Simultaneously changing SSTs in the Pacific and the North Atlantic (i.e., a joint response through changes in oceanic circulation) would likely induce a larger climatic response over WNA than those simulated here.

3.2 Regional Model

3.2.1 Glacial-Interglacial responses. Average January and July temperature, precipitation, and wind fields from the *Control* RegCM simulation (not shown) are consistent with the boundary forcing derived from GENESIS and are in relative agreement with long-term observations [Thompson *et al.*, 1998]. January temperatures over the northern Great Basin, however, are generally colder than observations by up to ~5°C. Simulated January temperatures over the SW are similarly colder than observed temperatures, but by $\leq 2^\circ\text{C}$. Precipitation in the January *Control* simulation generally agrees with observed values except over the coastal regions of the PNW and the northern Sierra Nevada where the RegCM underestimates precipitation rates by ~2 mm day⁻¹. (In December, simulated precipitation rates agree well with observed values over these regions.) The errors in simulated temperature and precipitation fields are attributed partly to the RegCM and partly to the aforementioned placement of circulation over WNA by GENESIS, which is consequently imposed on the RegCM through the lateral boundary conditions. July temperature and precipitation of the *Control* simulation are in relative agreement with observations over the model domain. Exceptions are found over the Rocky Mountains and the Mexican Plateau where local convective precipitation rates are up to several millimeters per day greater than averaged observed values.

Incorporating the large-scale circulation patterns from GENESIS into the RegCM produces glacial-interglacial (*MaxCold-Control*) climate anomalies over WNA similar in general pattern to those of the AGCM. During January, the flow aloft and at the surface (Plate 3b and 3c, *MaxCold-Control*) combine to generate drier-than-present conditions over the PNW and wetter-than-present conditions over the desert SW. Between the two extremes, a well-defined

precipitation gradient is evident across the Great Basin. The precipitation gradient suggests a mechanism whereby lakes to the south (e.g., Estancia, Owens) were at their maximum late-Pleistocene extents during the LGM while lakes in the northern Great Basin (e.g., Lahontan and Bonneville), though much larger than present, were not as large as their post-LGM maxima [Benson *et al.*, 1990; Hostetler and Benson, 1990]. Circulation changes aloft and at the surface in the *MaxCold* simulation also contribute to wetter-than-present conditions over much of the domain during July.

Glacial/interglacial temperature anomalies over the northern part of the domain are largest during January because anticyclonic flow off of the LIS sustains easterly winds across the PNW while farther to the east, northwesterly winds advect cold air off the LIS (Plate 3a *MaxCold-Control*). In the vicinity of Lakes Lahontan and Bonneville, lake heat storage increases air temperatures relative to those of the *Control* [Hostetler *et al.*, 1994]. In the SW, January LGM temperatures range from slightly lower to $\sim 3^{\circ}\text{C}$ higher than *Control* values. This apparent LGM warming reflects a cold bias in the *Control* simulation and warm air advection associated with the subtropical jet in the *MaxCold* simulation.

In contrast to January, July air temperatures over much of the domain are $4\text{--}8^{\circ}\text{C}$ colder than those in the control, with some areas along the margin of the LIS and over mountain glaciers being up to 16°C colder (Plate 3a). Slightly less cooling also occurs during spring and autumn (figures not shown). Mean annual temperatures of the *MaxCold* simulation are colder than the control by $4\text{--}5^{\circ}\text{C}$ or more over the PNW and northern part of the domain, $1\text{--}2^{\circ}\text{C}$ over the Sierra and the northern Great Basin, and $2\text{--}3^{\circ}\text{C}$ over the SW.

The simulated glacial/interglacial cooling over WNA is generally less than what is inferred from paleo-environmental indicators [Thompson *et al.*, 1993], particularly in winter. The lack of cooling in part is attributable to our use of CLIMAP SSTs which may be too warm in the midlatitudes of the eastern Pacific. Additional LGM cooling over WNA of $2\text{--}4^{\circ}\text{C}$ was simulated by Pollard and Thompson [1997] when fixed CLIMAP SSTs were replaced by a slab mixed layer ocean in GENESIS, (perhaps indicating improvement in the simulated wave pattern). We chose to begin our Heinrich event experiments with fixed SSTs so we could isolate and quantify the atmospheric responses associated with prescribed changes in the North Atlantic region, and it is likely that the use of lateral boundary conditions from a mixed-layer (or fully interactive) ocean simulation would produce further winter cooling in the *MaxCold* simulations. The magnitude and distribution of glacial/interglacial precipitation anomalies, in general, agree with paleoenvironmental reconstructions [Thompson *et al.*, 1993]. The pattern of opposing changes in wetness between the PNW and SW in particular is well simulated.

Although there are shortcomings in our simulated glacial/interglacial climate changes owing to limitations in the RegCM, and placement of synoptic-scale circulation features in the AGCM, the simulations provide a sufficient baseline against which the climatic variations of the canonical Heinrich event simulations can meaningfully be compared.

3.2.2 Heinrich event responses. Lowering the Laurentide ice sheet in the second (*MinCold*) phase of the Heinrich event experiments induces changes in the magnitude and distribution of pressure patterns aloft and at the surface, with attendant changes in upper level and surface winds over WNA (Plate 3b and 3c, *MinCold-MaxCold*). During January, there is a breakdown aloft in the effect of the glacial anticyclone and a reduction in the prominence of the split jet (in the AGCM), consequently intensifying the westerlies over the west coast and into the Great Basin while reducing the influence of the subtropical jet in the SW. At the surface there is also more westerly flow into the west coast in the *MinCold* simulation than in the *MaxCold*. In July, higher SLP is centered over Oregon and northern California in the *MinCold* simulation than in the *MaxCold*, and relative to the glacial/interglacial anomalies, northerly shore-parallel winds are further reduced along the PNW coastline. Near-shore winds are also reduced to a lesser degree along coast of southern California.

In contrast to glacial/interglacial changes in moisture patterns, precipitation increases by over 2 mm d^{-1} over the PNW, northern Sierras, and the northern Great Basin and decreases by up to 5 mm d^{-1} over the SW (Plate 3d, *MinCold - MaxCold*). Wetter conditions in the PNW in the *MinCold* simulation reverse the glacial/interglacial gradient and shift the line separating wetter from drier anomalies to the southwest. Differences between *MinCold* and *MaxCold* July precipitation rates are more heterogeneous than those of January, although the winter pattern of wetter conditions in the PNW and drier conditions in the SW is broadly maintained. The most obvious exception is a shift to wetter conditions over New Mexico which is associated with focused moisture advection from the Gulf of Mexico.

January temperatures in the second (*MinCold*) phase are up to $2\text{--}4^{\circ}\text{C}$ colder (than *MaxCold*) over parts of the PNW, the LIS, southward to the Great Basin, and much of the SW (Plate 3a). These areas of cooling are separated by an area of roughly equivalent warming extending eastward from eastern Oregon to the Yellowstone Plateau and southward into eastern New Mexico. Colder temperatures in the north are associated with increased cloud cover whereas cooling to the south is associated with advection of cold air from the north. The area of warming is produced by increased advection of warm air from the south and east, and to a lesser degree by elevated solar radiation levels from reduced cloud cover. July air temperatures are also up to 4°C lower over the PNW, reflecting strengthening of westerly flow and associated cloudiness. Warming

extending in a northwesterly direction from the SW is caused both by increased southerly advection and, as in January, to a lesser degree by elevated solar radiation levels.

In the third (*MinWarm*) stage of the canonical Heinrich event, in which increased North Atlantic SSTs are combined with a lower LIS, lower pressure forms aloft over the PNW (Plate 3b; *MinWarm-MaxCold*) in January causing upper-level wind flow to increase from a northwesterly direction over the eastern Pacific and west coast and to decrease to the east. At the surface, there is a general deepening of low pressure relative to both the *MaxCold* and *MinCold* simulations (Plate 3c; *MinWarm-MaxCold*). Lower surface pressure enhances shore-parallel flow along the northern and central coast and enhances westerly flow along the southern coast. In July, wind flow aloft in the *MinWarm* experiment is little changed relative to the *MaxCold* phase along the northern coast, but there is enhanced westerly flow that extends inland from the PNW across the northern Rocky Mountains. To the south there is strengthened anticyclonic flow aloft in the eastern Pacific and enhanced easterly flow over the southern SW and northern Mexico. At the surface, there are relatively minor changes in SLP and wind flow, except over and to the east of the northern Rocky Mountains.

January circulation changes in the *MinWarm* experiment (relative to the *MaxCold* experiment) generally result in slight redistribution of precipitation over WNA (Plate 3d). The exception is the wet area located along the southern edge of the low pressure cell centered over the PNW. In July, there is a mixed, and generally small, precipitation response with the largest change being wetter conditions over northern Mexico and the SW in response to the increased easterly flow aloft in the *MinWarm* experiment relative to the *MaxCold*.

Advection of cold air from the north by winds associated with low pressure aloft in the *MinWarm* experiment yields generally colder temperatures over WNA than those of the *MaxCold* experiment. Areas of cooling of up to 8°C are located over the northern portion of the domain. Cooling of 1-4°C occurs over the Sierras, the Great Basin and the SW (Plate 3a). July temperature anomalies are not as large as those of January, with cooling of up to 2°C over the PNW and about the same magnitude of warming east of the Northern Rocky Mountains.

3.3 Summary of Regional Model Results

As with the global climate simulations, the responses in WNA to the different phases of the canonical H2 event are spatially heterogeneous. A combination of large-scale controls and regional forcing yield regional responses that are reinforced, canceled, or reversed in the various phases of our H2 event. For example, the LGM pattern of relatively dry conditions in the PNW and wet conditions in the SW is attenuated or reversed in the *MinCold* phase.

Subsequent warming of the North Atlantic in the *MinWarm* phase leads to attenuated precipitation responses in some areas (PNW, Yellowstone Plateau, and SW), and produces different precipitation patterns in other areas (e.g., wetter conditions across Nevada, Utah, and eastern Colorado). The magnitudes of the climate anomalies in the *MinCold* and *MinWarm* phases range in value up to those of the glacial/interglacial, suggesting that millennial-scale climate changes such as Heinrich events may have been recorded by surface systems and processes (e.g., lakes, vegetation, glaciers, coastal upwelling). We explore the sensitivity of some of these systems in the following sections.

4. RESPONSE OF SURFACE SYSTEMS AND PROCESSES

4.1 Alpine glaciers and ice caps

Alpine glaciers and ice caps are sensitive and rapidly responding (response time on the order of $10\text{-}10^2$ yr) indicators of climate change [Paterson, 1994]. Geologic records from WNA suggest the possibility that glaciers responded not only to glacial/interglacial climate changes but also to millennial-scale climate variations [Clark and Bartlein, 1995]. The mass balance of a glacier is the difference between accumulation (precipitation falling as snow), and ablation which is governed by the surface energy balance (for which temperature is a proxy). For a particular glacier, the mass balance is thus a function of winter precipitation and summer air temperature. Empirical equations for computing glacier mass balance from temperature and precipitation have been developed from modern data sets [e.g., Leonard, 1989; Ohmura et al., 1992], and we have applied such a relation using output from RegCM to quantify the relative contribution of precipitation and temperature in maintaining LGM glaciers in WNA [Hostetler and Clark, 1997]. We follow that approach here to assess the sensitivity of glaciers to the climate variations of the H2 event.

At each model grid cell, total accumulation or snowfall is computed as the sum of precipitation (water equivalent) in the months in which the near-surface (2 m) air temperature is $\leq 0^\circ\text{C}$. Using average July-August air temperature values from the RegCM, we estimate ablation $A(T)$ from the empirical equation $A(T) = (T + 8.16)^{2.85}$ of Leonard [1989]. The mass balance at each grid cell is determined as the algebraic difference of accumulation and ablation. Based on an analysis of the interannual variability of mass balances of high-latitude glaciers at present, computed mass balances within the range of ± 750 mm yr⁻¹ are assumed to be in approximate equilibrium [Hostetler and Clark, 1997]. (Necessary topographic smoothing in the RegCM causes the elevations of mountains to be lower than actual elevations. We did not apply a lapse-rate correction to model air temperatures to account for differences in elevations, but such a correction would, in general, reduce estimated ablation and thus result in more positive mass

balances.)

The distribution of mass balance values for the *MaxCold* or LGM simulation (Plate 3e, *MaxCold*) are similar to those reported by *Hostetler and Clark* [1997]. Glaciers in the Northern Rocky Mountains and the Yellowstone Plateau that are generally controlled by temperature tend to have more positive mass balances than their precipitation-controlled counterparts located to the south and west. During the *MinCold* phase, the increase in precipitation (relative to the *MaxCold* phase) extending from the PNW to the eastern Yellowstone Plateau and southward into the Sierra Nevada and Wasatch Mountains in Utah drives the mass balance of glaciers there more positive, suggesting that these glaciers would have advanced during that phase of our canonical Heinrich event. Increased precipitation (accumulation) over the eastern Yellowstone Plateau during the *MinCold* phase is offset by warmer summer temperatures (ablation), subsequently yielding a more negative mass balance, suggesting possible glacier retreat. A common, large-scale climate event induced by lowering the LIS may thus have caused opposing responses over relatively short distances in this region (including northern Montana).

During the *MinWarm* phase, a different pattern of glacier response emerges (Plate 3e, *MinWarm-MaxCold*). Colder summer temperatures lead to reduced ablation and, combined with accumulation that is somewhat greater than the *MaxCold* experiment but less than that of the *MinCold* experiment, the mass balances of glaciers in the Cascades become less negative than in the *MaxCold* simulation. At the same time, reduced accumulation to the east causes a general trend toward more negative mass balances there. In the Sierra Nevada, Utah, and the central Rocky Mountains, increased accumulation and decreased ablation also yield more positive mass balances.

The sensitivity of alpine glaciers to millennial-scale climate variations simulated here suggests a complex response on two levels. First, over relatively short distances it might have been possible to record opposing glacier responses within each of the phases of a Heinrich event. Second, the direction of change to a subsequent phase may be of the same sign for the combinations of values of temperature and precipitation that lead to similar mass balances, or the direction of change can oppose that of the previous phase. This spectrum of possible responses suggests that geologic records of glacial advance and retreat during millennial-scale climate events may be difficult to correlate in a simple fashion, while remaining consistent with regional-scale climatic controls.

4.2 Lakes

Physical lake responses to climate change, including thermal structure (e.g., temperature, mixing, surface fluxes, ice cover) and area (level) also can be quantified by modeling. To evaluate thermal responses and interactions

with the atmosphere, an interactive lake model was used in RegCM to represent Lakes Bonneville and Lahontan, the largest of the pluvial lakes at the LGM. We can also assess the thermal response of other representative lakes not included in the RegCM by driving the lake model [*Hostetler and Bartlein*, 1990] “off line” with meteorological data from the RegCM simulations. Changes in levels are not explicitly computed in either case; rather we infer level changes from distribution of P-E as simulated by RegCM and the lake model.

Relative to the *MaxCold* simulation, the mean annual surface temperature of Lakes Lahontan and Bonneville are slightly colder ($\leq 0.5^{\circ}\text{C}$) in both the *MinCold* and *MinWarm* experiments. Changes in the water balance of the lake basins, which are dominated by changes in precipitation, are more substantial (Plate 3f). In the *MinCold* experiment, runoff from the land surface of the Lahontan basin increases by an average of 0.11 mm day^{-1} (relative to $.25 \text{ mm day}^{-1}$ in the *MaxCold* experiment) and P-E over the entire basin increases by an average of 0.18 mm day^{-1} (relative to a value of $-0.32 \text{ mm day}^{-1}$ in the *MaxCold* experiment). Over the Bonneville basin, in the *MinCold* phase, changes in P-E are smaller, with runoff increasing slightly by 0.06 mm day^{-1} (relative to a value of 0.48 mm day^{-1} in the *MaxCold* experiment) and P-E increasing by 0.11 mm day^{-1} (relative to a value of $-0.07 \text{ mm day}^{-1}$ in the *MaxCold* experiment). This tendency for rising lake levels in the Lahontan basin is sustained during the *MinWarm* stage of the Heinrich event with runoff and P-E both increasing by 0.15 mm day^{-1} relative to the *MaxCold* experiment. In the Bonneville basin, however, the tendency for rising lake levels in the *MinCold* phase is reversed in the *MinWarm* phase wherein the average runoff anomaly remains slightly positive (0.06 mm day^{-1}) but the average P-E anomaly is $-0.10 \text{ mm day}^{-1}$.

To provide some insight into the relative sensitivity of lakes of different sizes, climatic settings, and geographic locations, we obtained from the RegCM model the time series of daily values of the meteorological variables (air temperature, wind speed, humidity, longwave radiation, shortwave (solar) radiation) required to drive the lake model [*Hostetler and Bartlein*, 1990]. Sites were selected to represent Carp Lake (modeled depth of 4 m), Owens Lake (modeled depth of 60 m), and Lake Estancia (modeled depth of 10 m). The grid cell nearest to the actual location of the lakes was used as the target for the meteorological data. The simulated lakes are therefore not exact representations of the real lakes, but are sufficient to characterize first-order sensitivities.

The glacial/interglacial changes in the mean annual surface temperature of Owens and Estancia lakes are small (-1.4°C and $+1.4^{\circ}\text{C}$, respectively). Carp Lake has the largest temperature response of any of the simulated lakes. Because the lake is located in the area of prevailing, cold easterlies off the ice sheet, summer maximum and winter

minimum temperatures at the LGM (*MaxCold*) are $\sim 15^{\circ}\text{C}$ colder than present, and the annual average temperature is 11°C colder than the control. Changes in mean annual surface temperatures for all lakes are $\leq 1^{\circ}\text{C}$ for both the *MinCold* and *MinWarm* experiments relative to the *MaxCold* experiment.

As is the case for the large lakes, changes in the water balances of the smaller lakes are greater in relative magnitude than are temperature changes. During both the *MinCold* and *MinWarm* phases, simulated lake levels at Carp lake have a tendency to rise, with a greater rise occurring during the *MinCold* phase (Table 1). Lake Estancia, in contrast, tends to fall during both the *MinCold* and *MinWarm* phases. Owens Lake tends to fall during the *MinCold* phase and rise during the subsequent *MinWarm* phase. These lake responses reflect the broad patterns of a wet PNW and dry SW, along with shifts in location and steepness of the gradient between these extremes from one phase of the canonical Heinrich event to another.

Like alpine glaciers, the simulated response of lakes during different phases of our H2 event again suggest variable responses that are characterized primarily by changes in the water balance. Both Lakes Lahontan and Bonneville show increases in basin moisture during the *MinCold* phase (relative to the *MaxCold* phase), suggesting that over decades and centuries the lakes would expand. During the *MinWarm* phase, however, Lake Lahontan continues to support a lake larger than the *MaxCold* experiment, but a reduction in the moisture in the Bonneville basin would lead to a lake smaller than that of the *MaxCold* phase, and in opposition to the direction of change of Lake Lahontan. Similar pattern of variable response are demonstrated by the other lakes considered.

4.3 Vegetation

We use July soil moisture and seasonal temperature anomalies from the RegCM simulations to infer possible changes in vegetation during the various phases of our H2 event. Relative to the control, the *MaxCold* changes in July soil moisture are substantial and widespread over the model domain (Plate 3g). With the exception of coastal PNW, *MaxCold* soil moisture levels are higher than those of the control, particularly over the SW and into the Rocky Mountains. In the *MinCold* experiment, changes in precipitation result in a general reversal of the glacial/interglacial pattern of soil moisture anomalies, with moisture levels increasing in the PNW and decreasing in the SW, California, and the Great Basin. The pattern of soil moisture anomalies in the *MinWarm* experiment is more heterogeneous than that of the *MinCold* experiment. Soil moisture anomalies are positive, but of lower magnitude over the PNW, and a mix of positive and negative anomalies is found elsewhere. Northern and central California and the Sierra are drier, and a mix of drier and wetter areas is found in the Great Basin and SW.

The regional-scale patterns of the LGM-present (*MaxCold-Control*) anomalies of soil moisture and temperature are consistent with the broadscale patterns of paleoecological data [Thompson *et al.*, 1993] that show widespread replacement of forest by steppe across the northern half of WNA, and the reverse across the southern part of the region. Clear correlations between the paleoecological record and the simulated *MinCold-MaxCold* and *MinWarm-MaxCold* climate anomalies are more difficult to detect, even allowing for the large spatial heterogeneity evident in those anomaly patterns [see Whitlock and Grigg, this volume]. It is possible, however, that when the soil moisture anomalies are interpreted in light of other landscape scale controls of vegetation (e.g. soil type, proximity to physiographic barriers, see Whitlock and Bartlein, 1993), that consistency will emerge for the millennial-scale vegetation variations.

4.4 Coastal upwelling

A challenging aspect of understanding millennial scale climate changes is linking terrestrial and marine responses. Such a linkage is relatively straightforward in the North Atlantic region where strong (and consistent) marine and terrestrial responses are found for events such as the Younger Dryas climate reversal (H0). There are ample indications of millennial-scale climate events in marine and terrestrial records from the eastern Pacific and WNA, however, correlating these responses in time and space to events in the North Atlantic is more difficult in this distant region. Although we did not model oceanic circulation changes, we can quantify the relative sensitivity of wind-driven coastal upwelling to the various phases of the H2 event. Upwelling is a dominant control of marine productivity along the coast of WNA and changes in productivity recorded in marine cores potentially offer a path for associating terrestrial and marine responses to millennial-scale climate changes.

We use the method of Bakun and Nelson [1991] as modified by Ortiz *et al.* [1997] to compute curl of the wind stress on the 60-km grid of the RegCM. The magnitude and direction of the curl determines upwelling (cyclonic direction in the northern hemisphere) and downwelling (anticyclonic direction in the northern hemisphere). Monthly values of the northerly and westerly components of the surface wind (Plate 3c) for the summer (June through August) and winter (December through February) are used in the computation. Seasonal computations are made because there is a distinct seasonal cycle in upwelling along the coast of WNA. The spatial patterns of curl and thus of upwelling and downwelling for our *Control* simulation (not shown) compare favorably in both summer and winter with values computed from observed winds by Bakun and Nelson [1991]. The magnitude of the curl fields also compares well with those of Bakun and Nelson [1991] in summer, but we found the magnitude of our winter curl

values to be generally underestimated. We therefore corrected this underestimate, by scaling the *Control* RegCM winter wind fields by +20% to achieve better average agreement with the observed data. The scaling was applied to all subsequent winter curl computations, and thus does not affect the sign of anomalies among the various phases.

Along the coast and in the open ocean, substantial glacial/interglacial changes in curl of the wind stress and hence upwelling occur in winter and summer (Plate 3h). The patterns and magnitude of the changes compare favorably with those of *Ortiz et al.* [1997]. Off the PNW coast in January, upwelling is enhanced where easterly winds from the LIS dominate the *MaxCold* wind flow. To the south, there are areas of reduced upwelling off the coast of southern Oregon and northern California and along the southern California coast. In July, an area of reduced upwelling is located off the PNW and northern California coast, and farther to the south along southern California and the Santa Barbara basin. Enhanced upwelling occurs along and off shore of central California. Coastal upwelling changes are further quantified by the computed Ekman transport, which reflects the volume of offshore flow (Figure 2). In agreement with *Ortiz et al.* [1997], glacial/interglacial Ekman transport is reduced along the entire coastline, with the largest reductions occurring during summer.

In the *MinCold* experiment there is a mixed pattern of upwelling changes in winter, with the largest anomalies being located off the PNW coast and in the vicinity of the Santa Barbara basin (Plate 3h). Summer anomalies tend to reinforce the glacial/interglacial increase in the PNW, and reverse the pattern off California where increased upwelling is indicated. In the *MinWarm* phase, winter upwelling is reduced in the PNW and strengthened off the California coast and in the Santa Barbara basin, whereas summer anomalies are similar to those of the *MinCold* experiment. Winter Ekman transport in the *MinCold* experiment is reduced from 30°N to 36°N and increases to values exceeding the control, north of ~40°N, whereas summer transport exceeds the *MaxCold* from ~36°N to 43°N. In the *MinWarm* phase, Ekman transport is greater than that of the *MinCold* phase in the south, and about the same as the *MinCold* north of 36°. Summer transport values are greater than the *MaxCold* and *MinCold* phases from 34°N to 38°N, and less than previous values northward of 39°N.

Our curl computations suggest the possibility that changes in upwelling during a Heinrich event may be of sufficient magnitude to be recorded as changes in productivity in marine cores. The areas most likely to reflect the changes are the Santa Barbara basin, where winter upwelling is suppressed in both the *MinCold* and *MinWarm* phases, and off the PNW coast where an alternating pattern of increased and decreased upwelling is simulated. Interpretation of the results is not straightforward, however, because we cannot

isolate the contributions of changes in the location of the Alaskan gyre and the interplay between offshore and coastal upwelling. Nonetheless, our computed upwelling changes coupled, for example, with changes inferred changes in surface runoff suggest the existence of joint marine and terrestrial responses (e.g., the Columbia, Elk, and Santa Clara Rivers) during various phases of a Heinrich event.

5. DISCUSSION AND CONCLUSIONS

Our modeling study allows us to decompose global, millennial-scale climate variations into synoptic and regional components by using a suite of models to assess the response of global climate changes on regional and local processes in WNA. At the global scale, our canonical Heinrich event is transmitted to WNA primarily by the effects of topographic and thermal forcing of the LIS and secondarily by transmission from the North Atlantic region through circum-polar circulations. In WNA, synoptic-scale responses of precipitation and temperature are induced by changes in the location and strength of large-scale atmospheric pressure patterns and their influence on wind flow at the surface and aloft. Changes in the synoptic-scale climatology simulated by the GCM in the *MinCold* and *MinWarm* phases of the Heinrich event are downscaled by the higher resolution regional climate model that portrays more variable topographic complexity.

Simulated millennial-scale climate responses in WNA are characterized primarily by changes in precipitation patterns, and secondarily by changes in temperature and wind flow both within a particular phase and among the various phases. Spatially, the responses within a particular phase can be of opposite sign (e.g., the pattern of wet PNW and dry SW in the *MinCold* simulation), and these responses can reinforce, cancel, or reverse responses of previous or subsequent phases (e.g., the wet PNW-dry SW pattern of the *MinCold* simulation is opposite that of the *MaxCold* simulation). The potentially complex pattern of regional climate change that ensues from changes in global boundary conditions suggests caution when attempting to infer millennial-scale climate variations from geologic records of WNA. Our process modeling underscores this cautionary statement.

Relative to the LGM, during the *MinCold* phase simulated alpine glaciers would advance in the PNW, and retreat in the Sierra and Rocky Mountains. Moreover, there is an indication that some areas such as the Yellowstone region could have registered opposing responses. In the *MinWarm* phase, simulated glaciers would retreat in the PNW and Rocky Mountains while advances would occur in the Sierra. These variable responses are also evident in changes in simulated lake level, vegetation and upwelling. In addition, during some phases, different systems register opposite responses. For example, in the *MinWarm* phase, glacier advances in the Sierra are indicated, yet negative soil moisture anomalies west of the Sierra suggest a

possible vegetation shift to more xeric taxa. Similarly, opposing responses are evident in the PNW and northern Rocky Mountains.

Our modeling study has limitations. First, the canonical Heinrich event patterned after H2 was prescribed as a linear progression of what are thought to be primary components of Heinrich events in general, and it is likely that a collapse of the LIS and changes in thermohaline circulation were not discrete. In addition, we did not change SSTs in the Pacific, although it is likely that some oceanic teleconnection existed through which SSTs in the Pacific did change in response to variations in North Atlantic thermohaline circulation. Changing SSTs in the Pacific in general, or along the coast of WNA in particular, would substantially affect our simulated regional climate. Finally, our RegCM simulations are 4 years long. Over this relatively short period, interannual variability in the climate (or, actually, in the weather) can be large relative to changes among the simulations. For the domain of the RegCM, the envelope of interannual variability is ultimately limited by the driving AGCM, and any given 4-yr period in an AGCM simulation usually differs from other 4-yr periods. In our GENESIS simulations, we achieved significant changes in climate for each phase of the H2 event in 15-yr. simulations. It is therefore likely that we would also achieve significance in our RegCM simulations if they were run out for the same 15 years, but the computational needs for 60 years of RegCM simulation are prohibitive. These limitations notwithstanding, our modeling study demonstrates that millennial-scale climate responses in WNA derived from changes in a combination of circulation features occurring at a variety of scales, could have left a complex signature in the geologic record of terrestrial and marine systems.

Acknowledgments. We thank P. Clark, P. Fawcett, D. Zahnle for their reviews and comments. This research was supported by the U.S. Geological Survey and National Science Foundation grant ATM-9532974 to the University of Oregon. Model simulations were conducted at NCAR.

P.J. Bartlein, Department of Geography, University of Oregon, Eugene, OR 97403 (bartlein@oregon.uoregon.edu)

S.W. Hostetler, U.S. Geological Survey, 200 SW 35th St, Corvallis, OR 97333 (steve@ucar.edu)

REFERENCES

- Bakun, A. and C.S. Nelson, The seasonal cycle of wind-stress curl in subtropical eastern boundary current regions, *J. Phys. Oceanogr.*, *21*, 1815-1834, 1991.
- Bartlein, P.J., K.H. Anderson, P.M. Anderson, M.E. Edwards, C.J. Mock, R.S. Thompson, R.S. Webb, T.W. Webb, C. Whitlock, Paleoclimate simulations for North America over the past 21,000 years: Features of the simulated climate and comparisons with paleoenvironmental data, *Quat. Sci. Rev.*, *17*, 549-586, 1998.
- Behl, R.J., and J.P. Kennett, Brief interstadial events in the Santa Barbara Basin, NE Pacific, during the last 60 kyr, *Nature*, *379*, 243-246, 1996.
- Benson, L.V., J.W. Burdett, M. Kashgarian, S.P. Lund, F.M. Philipps, and R.O. Rye, Climatic and hydrologic oscillations in the Owens Lake basin and adjacent Sierra Nevada, California, *Science*, *274*, 746-749, 1996.
- Benson, L.V., S.P. Lund, J.W. Burdett, M. Kashgarian, T.P. Rose, J.P. Smoot, and M. Schwartz, Correlation of late-Pleistocene lake-level oscillations in Mono Lake, California, with North Atlantic climate events, *Quat. Res.*, *49*, 1-10, 1998.
- Benson, L.V., D.R. Currey, R.I. Dorn, K.R. Lajoie, C.G. Oviatt, S.W. Robinson, G.I. Smith, S. Stine, Chronology of expansion and contraction of four Great Basin lakes, *Paleogeog., Paleoclim., Paleocol.*, *78*, 241-286, 1990.
- Berger, A. Long-term variations of caloric solar radiation resulting from the earth's orbital elements, *Quat. Res.*, *9*, 139-167, 1978.
- Clark, P.U. and P.J. Bartlein, Correlation of late-Pleistocene glaciation in the western United States with North Atlantic Heinrich events, *Geology*, *23*, 483-486, 1995.
- COHMAP Members, Climatic changes of the last 18,000 years: Observations and model simulations, *Science*, *241*:1043-1052, 1988.
- Cortijo, E., L. Labeyrie, L. Vidal, M. Vautravers, M. Chapman, J.-C. Duplessy, M. Elliot, M. Arnold, J.-L. Turon, and G. Auffret, Changes in sea surface hydrology associated with Heinrich event 4 in the North Atlantic Ocean between 40° and 60°N, *Earth Planet. Sci. Lett.*, *146*, 29-45, 1997.
- CLIMAP Project Members, Seasonal reconstruction of the earth's surface at the last glacial maximum. *Geol. Soc. Amer. Map & Chart Series MC-3*, 1981.
- Giorgi, F., M.R. Marinucci, G.T. Bates, Development of a second-generation regional climate model (RegCM2). Part I: Boundary-layer and radiative transfer processes, *Monthly Weath. Rev.*, *121*, 2794-2813, 1993a.
- Giorgi, F., M.R. Marinucci, G.T. Bates, Development of a second-generation regional climate model (RegCM2). Part II: Convective processes and assimilation of lateral boundary conditions, *Monthly Weath. Rev.*, *121*, 2814-2832, 1993b.
- Hostetler, S. W. and P.U. Clark, Climatic controls of western U.S. glaciers at the last glacial maximum, *Quat. Sci. Rev.*, *16*, 505-511, 1997.
- Hostetler, S. W. and P.J. Bartlein, Modeling climatically determined lake evaporation with application to simulating lake-level variations of Harney-Malheur Lake, Oregon. *Water Res. Res.* *26*, 2603-2612, 1990.
- Hostetler, S. W., P.U. Clark, P.J. Bartlein, A.C. Mix, and N.J. Pisias, Atmospheric transmission of North Atlantic Heinrich events, *J. Geophys Res.*, *104*, 3947-3952, 1999.
- Hostetler, S.W., F. Giorgi, G.T. Bates, and P.J. Bartlein, Lake-atmosphere feedbacks associated with paleolake Bonneville and Lahontan, *Science*, *263*, 665-668, 1994.
- Hostetler S. W. and L.V. Benson, Paleoclimatic implications of the high stand of Lake Lahontan derived from models of evaporation and lake level, *Clim. Dyn.*, *4*, 207-217, 1990.
- Hostetler S. W. and L. V. Benson, Stable isotopes of oxygen and hydrogen in the Truckee River-Pyramid Lake surface-water system. 2. A predictive model of $\delta^{18}\text{O}$ and $\delta^2\text{H}$ in Pyramid Lake, *Limnol. Oceanogr.*, *39*, 356-364, 1994.
- Leonard, E.M., Climatic change in the Colorado Rocky Mountains: estimates based on modern climate at late Pleistocene equilibrium lines, *Arc. Alp. Res.*, *21*, 245-255, 1989.
- Licciardi, J.M., P.U. Clark, J.W. Jenson, and D.R. MacAyeal, Deglaciation of a soft-bedded Laurentide Ice Sheet, *Quat. Sci. Rev.*, *17*, 427-448, 1998.
- Lund, D.C., and A.C. Mix, Millennial-scale deep water oscillations: Reflections of the North Atlantic in the deep Pacific from 10 to 60 ka, *Paleoceanography*, *13*, 1-19, 1998.
- Manabe, S. and A.J. Broccoli, The influence of continental ice sheets on the climate of an ice age, *J. Geophys. Res.* *90*, 2167-2190, 1985.
- Ohmura, A., P. Kasser, and M. Funk, Climate at the equilibrium line of glaciers, *J. Glaciol.*, *38*, 397-411, 1992.
- Ortiz, J., A. C. Mix, S. W. Hostetler, and M. Kashgarian, The California Current of the last glacial maximum: Reconstruction at 42°N based on multiple proxies, *Paleoceanography*, *12*, 191-205, 1997.
- Oviatt, C.G., Lake Bonneville fluctuations and global climate change, *Geology*, *25*, 155-158, 1997.
- Paterson, W.S.B., *The Physics of Glaciers*. Pergamon Press, Oxford, 480 pp., 1994.
- Peltier, W.R., Ice age paleotopography, *Science*, *265*, 195-201, 1994.
- Phillips, F.M., M.G. Zreda, L.V. Benson, M.A. Plummer, D. Elmore, and P. Sharma, Chronology for fluctuations in late Pleistocene Sierra Nevada glaciers and lakes, *Science*, *274*, 1996.
- Pollard, D. and S.L. Thompson, Climate and ice-sheet mass balance at the Last Glacial Maximum from GENESIS version 2 global climate model, *Quat. Sci. Rev.*, *16*, 841-863, 1997.
- Rind, D., Components of Ice Age circulation, *J. Geophys. Res.*, *92*, 4241-4281, 1987.
- Small E.E., L.C. Sloan, F. Giorgi, and S. W. Hostetler, Simulating the regional water balance of the Aral Sea with a coupled regional climate-lake model, *J. Geophys. Res.*, in press.
- Thompson, R.S., C. Whitlock, P.J. Bartlein, S.P. Harrison, W.G. Spaulding, Climatic changes in the western United States since 18,000 yr B.P., in *Global Climates Since the Last Glacial Maximum*, edited by H.E. Wright, Jr., J.E. Kutzbach, T. Webb, W.F. Ruddiman, F.A. Street-Perrott, and P.J. Bartlein, pp. 468-513, University of Minnesota Press, Minneapolis, 1993.
- Thompson, R.S., S.W. Hostetler, P.J. Bartlein, and K.H. Anderson, A strategy for assessing potential future changes in climate, hydrology, and vegetation in the Western United States, *U.S. Geological Survey Circular 1153*, 20 pp., 1998.
- Weaver, A.J., Eby, M., Fanning, A.F., and Wiebe, E.C., Simulated influence of carbon dioxide, orbital forcing, and ice sheets on the climate of the last glacial maximum, *Nature*, *394*, 847-853, 1998.
- Whitlock, C. and Bartlein, P.J., Spatial variations of Holocene climatic change in the Yellowstone region. *Quat. Res.*, *39*, 231-238, 1993.

REGIONAL RESPONSES TO A HEINRICH EVENT, WESTERN NORTH AMERICA

Whitlock, C. and P.J. Bartlein, Vegetation and climate change in northwest America during the past 125 kyr, *Nature*, 388, 57-61, 1997.

Whitlock, C. and L.D. Grigg, Paleocological evidence of Milankovitch and sub-Milankovitch climate variations in the Western US during the late Quaternary, in *Mechanisms of Millennial-Scale Global Climate Change*, edited by P.U. Clark, R.S. Webb, L.D. Keigwin, this volume.

Wright, H.E., Jr., J.E. Kutzbach, T. Webb, W.F. Ruddiman, F.A. Street-Perrott, and P.J. Bartlein, editors, *Global Climates Since the Last Glacial Maximum*, University of Minnesota Press, Minneapolis, 569 pp, 1993.

Table 1. Changes in annual water balance components of selected lake locations. The changes are relative to the *MaxCold* simulation. Δr : change in runoff; $\Delta P-E$: change in net basin moisture; ΔE_{lake} : change in lake evaporation, Lake Level: tendency to rise (+) or fall (-). Units of Δr , $\Delta P-E$, and ΔE_{lake} mm day⁻¹.

Lake	MinCold		MinWarm		ΔE_{lake}		Lake Level	
	Δr	$\Delta P-E$	Δr	$\Delta P-E$				
Carp	0.3	0.3	0.1	0.1	0.0	0.0	++	+
Owens	-0.1	-0.2	0.2	0.0	0.1	0.0	-	+
Estancia	-0.2	-0.1	-0.1	-0.2	0.0	0.1	-	-

FIGURE CAPTIONS

Figure 1. Representation of the topography of western North America at different model resolutions. A: T31 (3.75° × 3.75°) as in GENESIS; B: 2° × 2° as in the land surface scheme LSX in GENESIS; C: ~0.5° × 0.5° (60 km × 60 km) as in RegCM. Areal coverage is approximately the same for each surface map and the vertical scales are exaggerated.

Plate 1. Present and LGM land surface types used in the RegCM simulations.

Plate 2. Anomalies of selected climate fields from GENESIS simulations. The left-hand column is glacial/interglacial (*MaxCold* minus *Control*), the middle column is the first phase of the H2 event (*MinCold* minus *MaxCold*), and the right-hand column is the second phase of the H2 event (*MinWarm* minus *MaxCold*). A: Surface (2 m) air temperatures for winter (DJF) and summer (JJA); B: ~500 mb wind vectors and wind magnitudes (shown in color and computed as $\sqrt{u^2+v^2}$, where u and v are the northerly and westerly components of the wind, respectively); C: Sea level pressure (shown in color) and surface wind vectors; D: Precipitation minus evaporation. The anomalies are computed from 12-year averages of the GENESIS simulations.

Plate 3. Anomalies of climate fields from the RegCM simulations (left-hand column) and related surface process responses (right-hand column). The order of presentation within both columns is glacial/interglacial (*MaxCold* minus *Control*), the first phase of the H2 event (*MinCold* minus *MaxCold*), and the second phase of the H2 event (*MinWarm* minus *MaxCold*). A: Surface (2 m) air temperatures for winter (DJF) and summer (JJA); B: ~500 mb wind vectors and wind magnitudes (shown in color and computed as $\sqrt{u^2+v^2}$, where u and v are the northerly and westerly components of the wind, respectively); C: Sea level pressure (shown in color) and surface wind vectors; D: Precipitation; E: Annual mass balance of alpine glaciers; F: Annual precipitation minus evaporation from the RegCM; G: July soil moisture from the RegCM; H: January and July wind-stress curl. The anomalies are based on 4-year averages from the RegCM simulations.

Figure 2. Offshore Ekman transport for *Control*, *MaxCold* (LGM), *MinCold*, and *MinWarm* phases of the H2 event. The transport values are computed using the northerly and westerly components of the surface winds from the RegCM simulations as an approximation to actual shore-parallel winds.

Topography of WNA at Various Model Resolutions

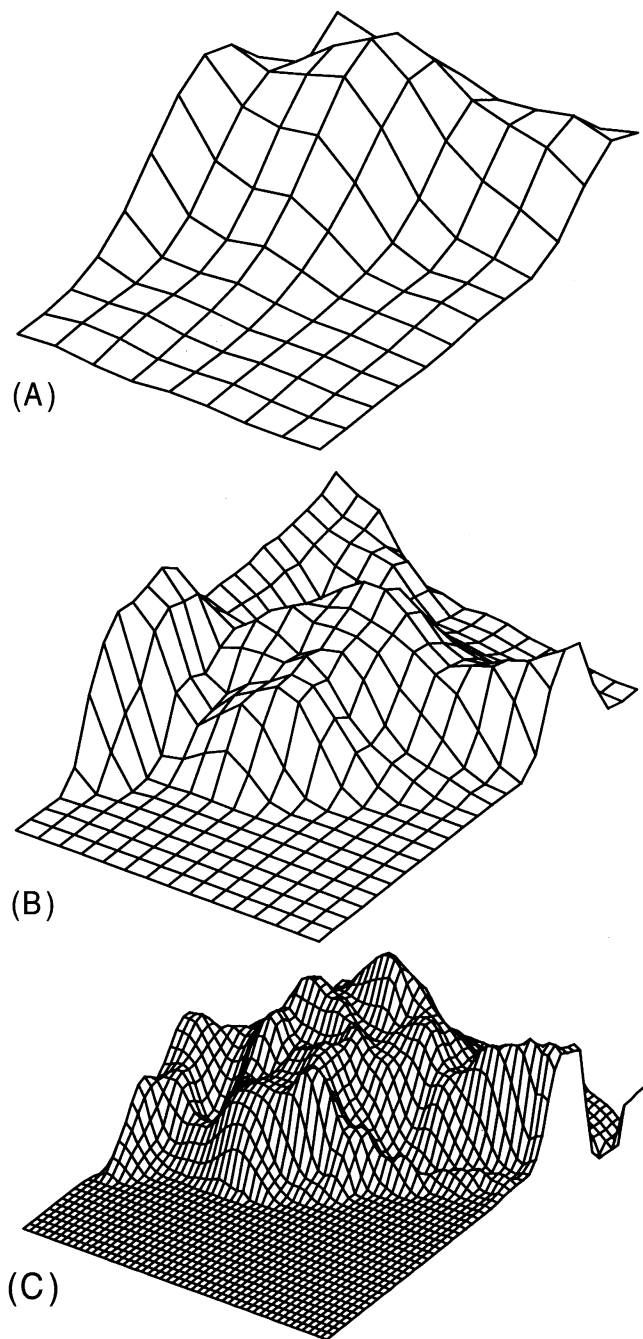


Figure 1. Representation of the topography of western North America at different model resolutions. A: T31 ($3.75^\circ \times 3.75^\circ$) as in GENESIS; B: $2^\circ \times 2^\circ$ as in the land surface scheme LSX in GENESIS; C: $\sim 0.5^\circ \times 0.5^\circ$ (60 km \times 60 km) as in RegCM. Areal coverage is approximately the same for each surface map and the vertical scales are exaggerated.

Present Vegetation

LGM Vegetation

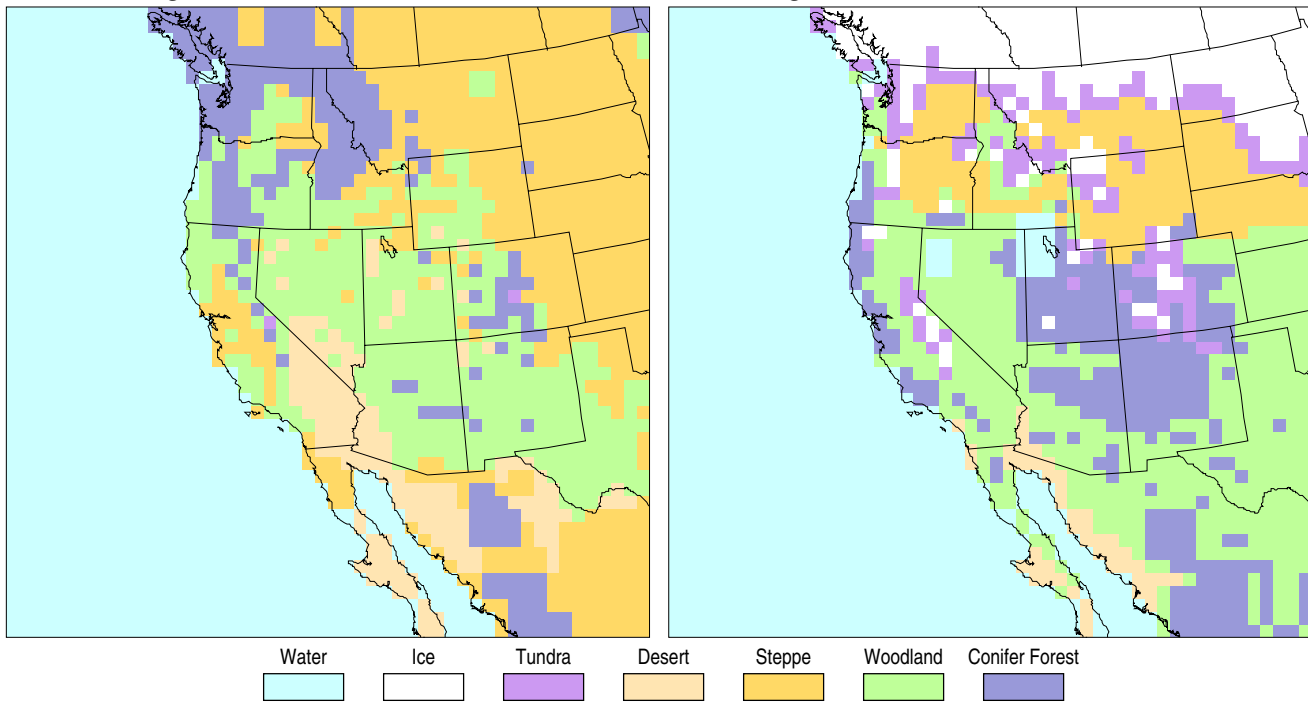
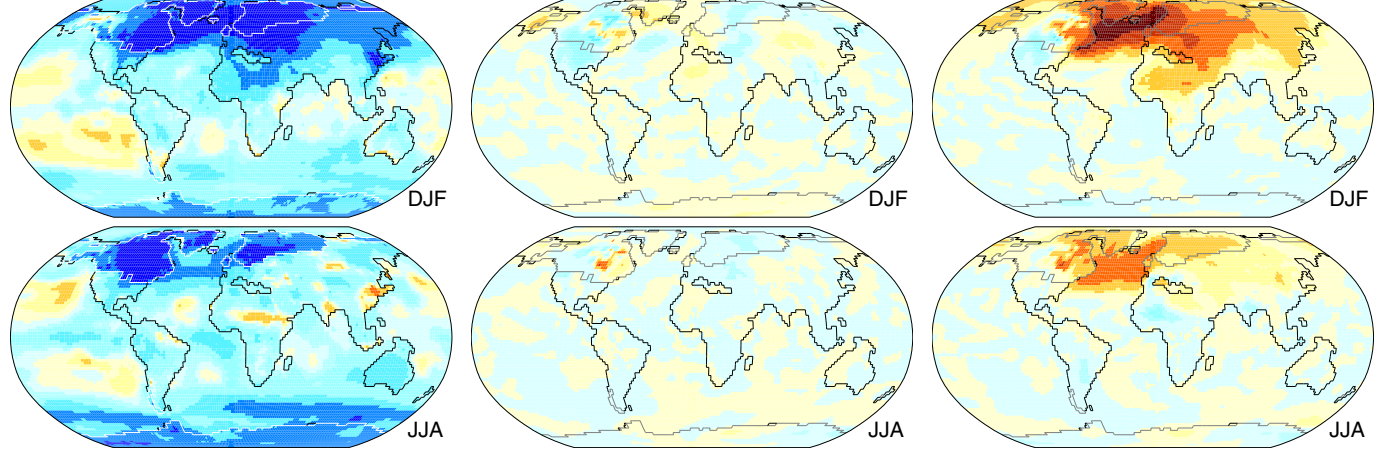
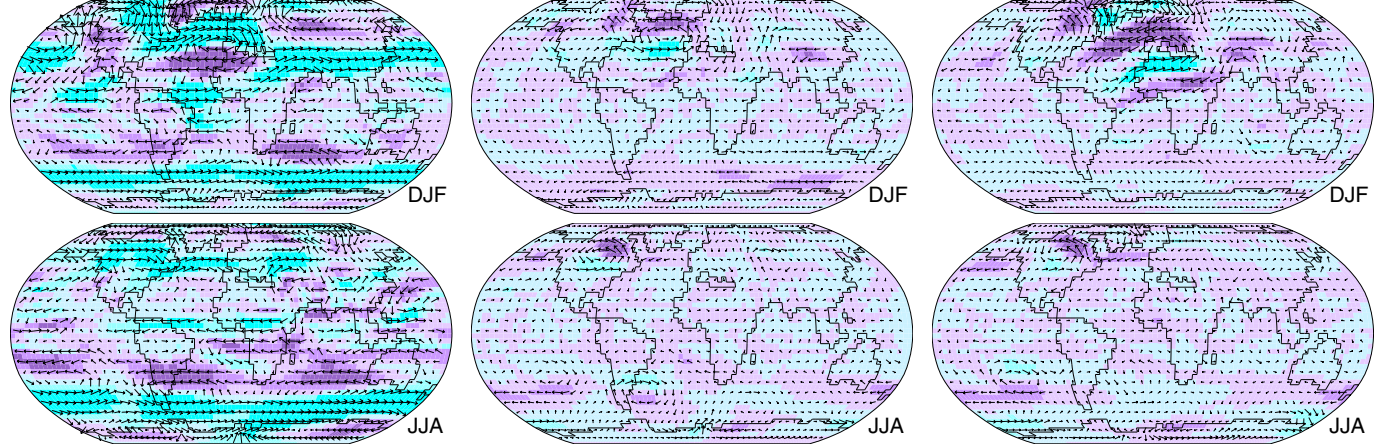


Plate 1. Hostetler, S.W. and P.J. Bartlein (1999) Simulation of the potential responses of regional climate and surface processes in western North America to a canonical Heinrich event. In P.U. Clark, R.S. Webb and L.D. Keigwin (eds.) *Mechanisms of Global Climate Change at Millennial Time Scales*, Geophysical Monograph 112, American Geophysical Union, pp. 313-327.

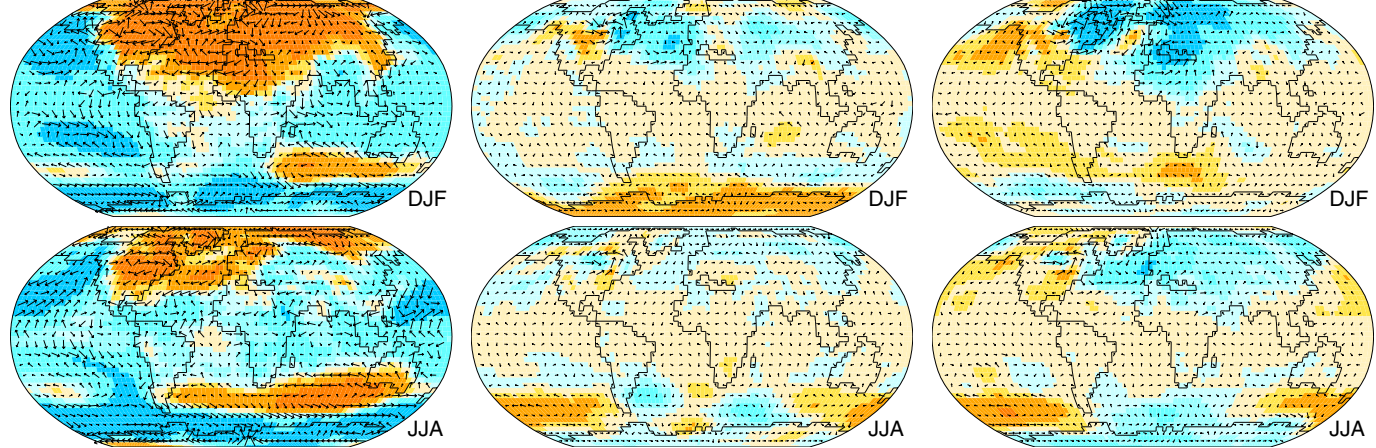
2m-Air Temperature Anomalies (a)



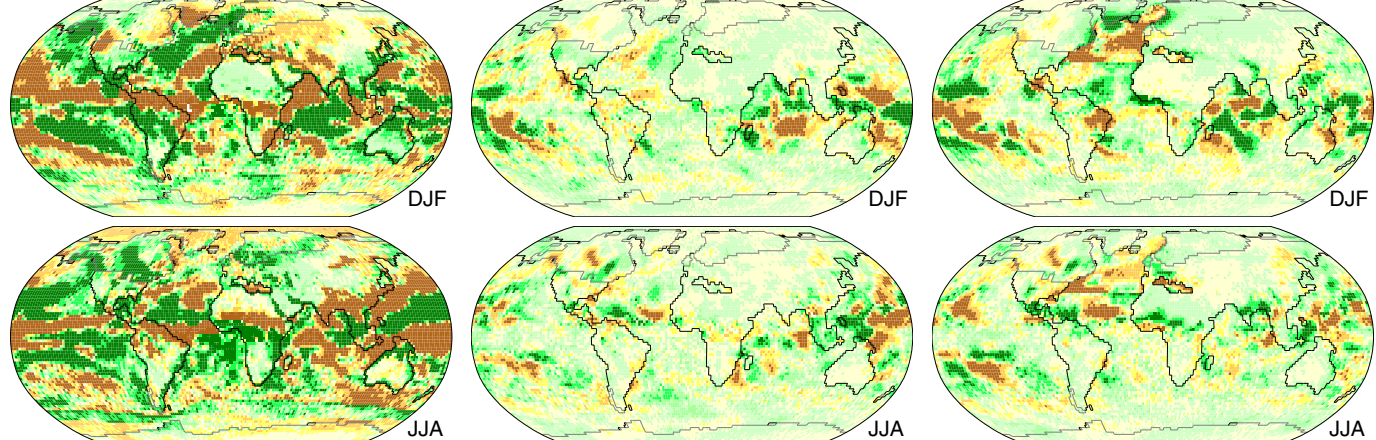
Upper-Level Wind Anomalies (b)



SLP and Surface-Wind Anomalies (c)



Precipitation - Evaporation Anomalies (d)



LGM Anomaly (MaxCold - Control)

(MinCold - MaxCold)

(MinWarm - MaxCold)

Plate 2. Hostetler, S.W. and P.J. Bartlein (1999) Simulation of the potential responses of regional climate and surface processes in western North America to a canonical Heinrich event. In P.U. Clark, R.S. Webb and L.D. Keigwin (eds.) *Mechanisms of Global Climate Change at Millennial Time Scales*, Geophysical Monograph 112, American Geophysical Union, pp. 313-327.

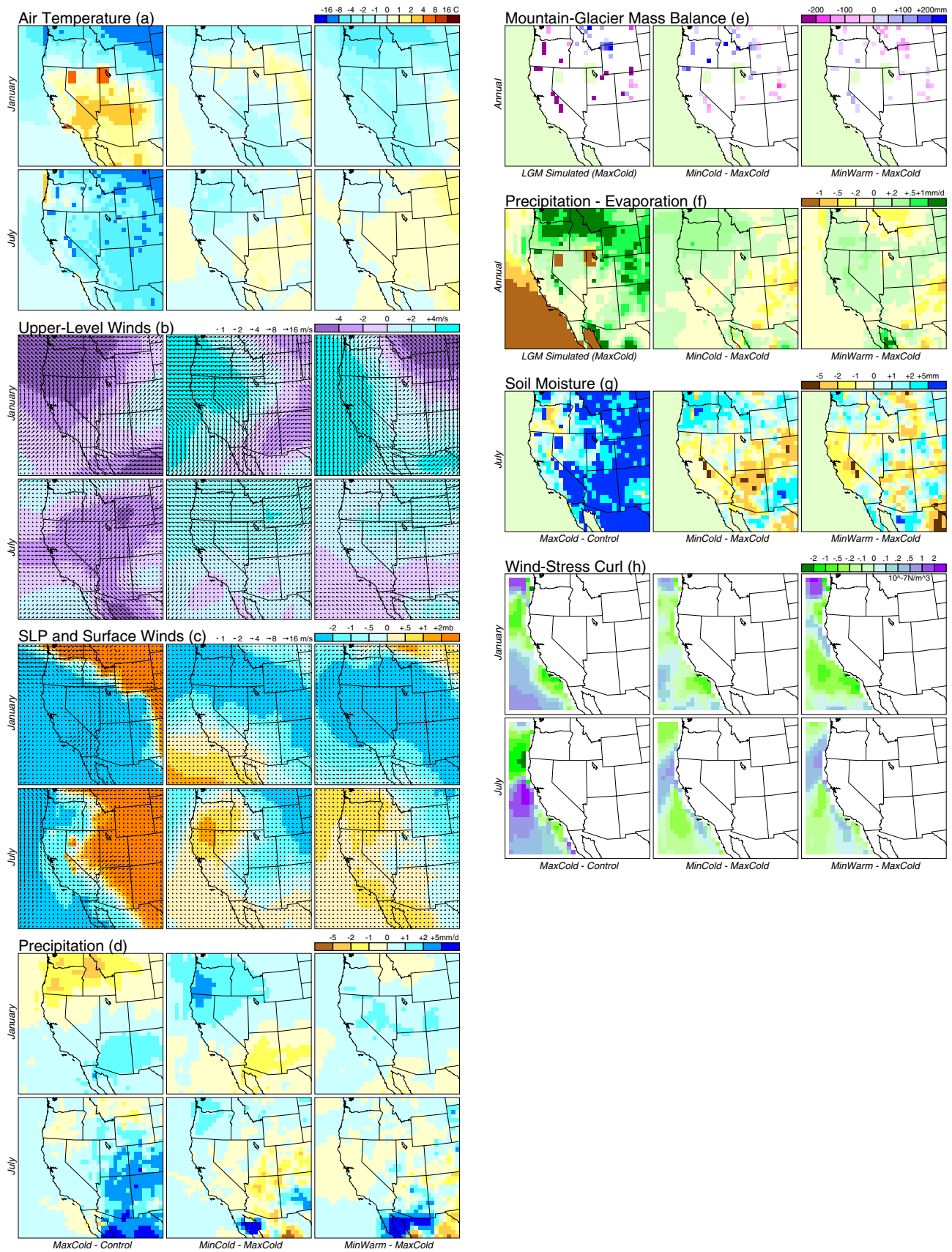


Plate 3. Hostetler, S.W. and P.J. Bartlein (1999) Simulation of the potential responses of regional climate and surface processes in western North America to a canonical Heinrich event. In P.U. Clark, R.S. Webb and L.D. Keigwin (eds.) *Mechanisms of Global Climate Change at Millennial Time Scales*, Geophysical Monograph 112, American Geophysical Union, pp. 313-327.

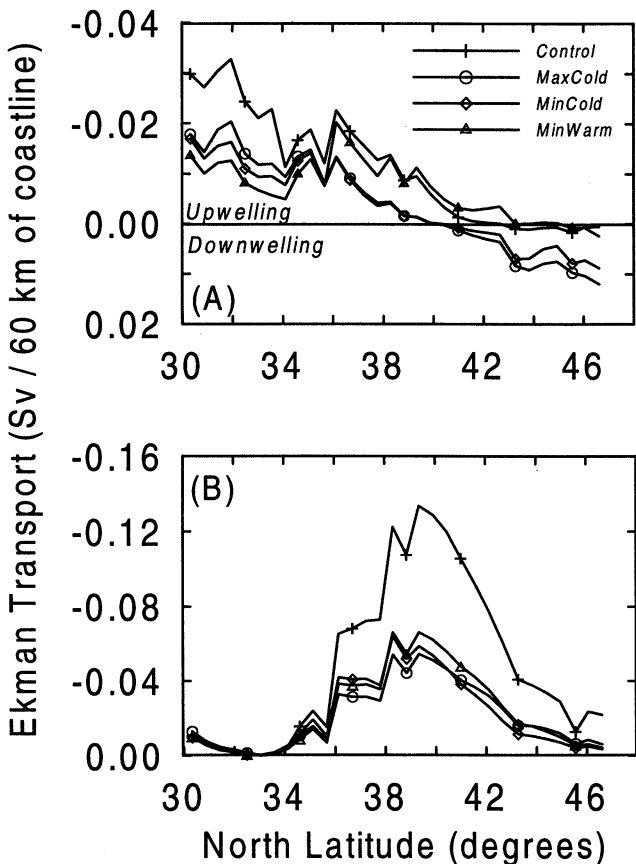


Figure 2. Offshore Ekman transport for *Control*, *MaxCold* (LGM), *MinCold*, and *MinWarm* phases of the H2 event. The transport values are computed using the northerly and westerly components of the surface winds from the RegCM simulations as an approximation to actual shore-parallel winds.